Inorganica Chimica Acta, *124* (1986) 187–198

Electrochemical Investigations of Platinum–Methyluracil–Blue and the Related Binuclear Complex $[(NH_3)_2Pt(MeU)_2Pt(NH_3)_2](NO_3)_2$

TORE RAMSTAD*, J. DEREK WOOLLINS** and MICHAEL J. WEAVER

Department of Chemistry, Purdue University, West Lafayette, Ind. 47907, U.S.A.

(Received November 25, 1985; revised March 18, 1986)

Abstract

The redox behavior of the head-to-head bis(μ-(1-methyluracilato-N^3,O^2)-bis(*cis*-diammine platinum-(II)) dinitrate, PtMeU, and platinum 1-methyluracil blue, PtMeUB, was studied by cyclic voltammetry (CV), rotating disk voltammetry (RDV), and controlled-potential coulometry (CPC). Redox titrimetry, electrochemistry/electron paramagnetic resonance spectroscopy (EPR), and liquid chromatography (LC) served as complementary techniques. The former reactant exhibits two-step electro-oxidation, consistent with the formation of a mixed-valence Pt(II, III) state en route to Pt(III, III). The latter also appears to oxidize to a uniform Pt(III) state. Although the oxidative–reductive electrochemistry of both reactants exhibits chemical reversibility, the heterogeneous electron-transfer kinetics are notably sluggish. The latter appears to be associated with the formation of an inhibiting film on the electrode surface. A slow conversion of PtMeU to a PtMeUB-like state was revealed by CV and LC. The complex, oligomeric nature of PtMeUB was revealed by means of gradient LC examination. Comparing oxidative and reductive electrolysis curves for PtMeUB yielded an average platinum oxidation state of 2.08. All observed behavior for PtMeUB, as well as for PtMeU, is accounted for by invoking +2 and +3 oxidation states for platinum; redox titrimetry using Ce(IV) revealed inconsequential oxidation of both of these systems beyond the III state. An estimate of molecular weight for the platinum blue was made by employing RDV in conjunction with the Einstein–Stokes equation.

Introduction

The discovery by Rosenberg and coworkers of the potency of platinum pyrimidine blues as antitumor agents ushered in a new era of research into platinum-bearing anticancer drugs. These compounds have proved effective in laboratory trials against a wide variety of tumors [1, 2] while also being less toxic than their precursor *cis*-$Pt(NH_3)_2Cl_2$ [3]. Quite apart from their potential as antitumor agents, the platinum blues have attracted widespread interest. They are mixed-valent, paramagnetic, cationic chains in which the platinum atoms are coordinated by bridging amidate ligands, their coordination shells generally being completed by bonding to ammine groups. Most structural knowledge stems from inference to a crystalline synthetic analog, platinum α-pyridone blue [4], although there has recently been a report on one crystalline form of platinum methyluracil blue [5].

Due to the mixed-valent state of platinum blues they are inviting candidates for electrochemical examination, yet to our knowledge no such investigations on platinum pyrimidine blues have been conducted. Limited studies have, however, been carried out on several binuclear α-pyridone complexes [6]. Redox studies on blues and precursors involving the use of Ce(IV) titrimetry have been more numerous [4, 7–9] with oxidation states of 2, 3 and 4 for platinum having been invoked to rationalize the titration data. Restriction to the lower two oxidation states has been sufficient to account for the observed behavior of pyrimidine blues.

We report here on electrochemical and related studies conducted on platinum 1-methyluracil blue, PtMeUB, and on its simpler head-to-head congener, PtMeU: bis(μ-(1-methyluracilato-N^3,O^2)-bis(*cis*-diammineplatinum(II)) dinitrate, $[(NH_3)_2Pt(MeU)_2Pt(NH_3)_2](NO_3)_2$ (MeU = 1-methyluracil anion). A possible structure for the oligomeric PtMeUB, one which

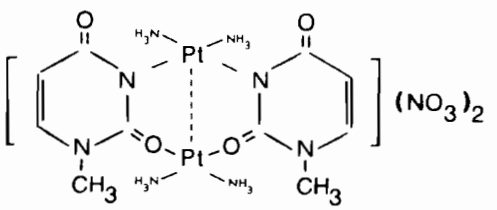

PtMeU

*Taken in part from M.Sc. Thesis of T. Ramstad, Michigan State University, 1983.

**Present address: Department of Chemistry, Imperial College of Science and Technology, South Kensington, London SW7 2AY, England.

0020-1693/86/$3.50

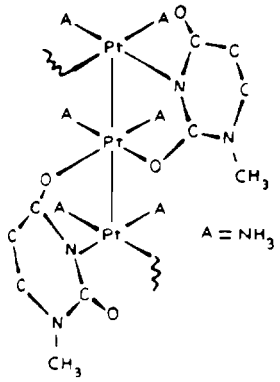

PtMeUB

mimics that proposed for platinum uracil blue [9], is shown above. One interesting feature of these studies is the preparation via controlled potential electrolysis of mixed-valence, head-to-head *cis*-$[(NH_3)_2Pt(MeU)_2Pt(NH_3)_2](ClO_4)_3$, 'Pt(ox)MeU'.

Experimental

PtMeUB, PtMeU, *cis*-$Pt(NH_3)_2(MeU)_2 \cdot 2H_2O$ and $[(NH_3)_2Pt(OH)_2Pt(NH_3)_2](NO_3)_2$ were prepared as previously described [1, 10]. To prepare PtMeU, *cis*-$Pt(NH_3)_2Cl_2$ was stirred overnight in the dark with $AgNO_3$. After removal of AgCl by filtration, $Pt(NH_3)_2(H_2O)_2^{2+}$ was treated with *cis*-$Pt(NH_3)_2(MeU)_2 \cdot 2H_2O$ [10] and its pH adjusted to 3.0 with HNO_3. The solution was stoppered and stored overnight. The volume was then reduced to 5 ml and the product filtered off, washed with ice cold water, and dried *in vacuo*. To prepare PtMeUB, *cis*-$Pt(NH_3)_2Cl_2$ was hydrolyzed overnight in water using $AgNO_3$. The diaquo product formed was subsequently reacted with 1-methyluracil at a pH of 7.8. The PtMeUB formed slowly over a several days incubation period at 40 °C. The reaction mix was then cooled to 0 °C and the resulting blue solid collected by filtration. Reprecipitation of the blue powder was accomplished with ethanol. (Since the completion of this work, a report has appeared on an alternate synthetic procedure which has yielded a structurally-characterizable, crystalline platinum methyluracil blue [5]).

The purity of PtMeU was established by ion-pair, reversed phase liquid chromatography (IPRPLC, see Results and Discussion). *Anal.* Found: C, 14.40; H, 2.42; N, 16.30; O, 19.84; Pt, 44.4. Calc.: C, 14.42; H, 2.64; N, 16.83; O, 19.23; Pt, 46.9%. The oligomeric nature and distribution of PtMeUB were demonstrated by gradient IPRPLC (see below). PtMeUB. *Anal.* Found: C, 14.67; H, 2.57; N, 13.89; O, not determined; Pt, 44.7.

Electrochemistry

The primary electrochemical techniques used were cyclic voltammetry (CV), rotating disk voltammetry (RDV), and controlled-potential coulometry (CPC) [11]. Platinum was most commonly used as the working electrode, usually configured as a flag of roughly 4 mm^2 area, although initial survey scans also made use of other electrode materials (glassy carbon, gold and mercury). The surface preparation of Pt consisted of acid cleaning followed by flame heating just prior to use. A standard 3-electrode arrangement was employed with a platinum wire serving as the auxiliary electrode and a saturated sodium chloride–calomel reference electrode (SSCE). The supporting electrolyte was either 0.1 M $NaClO_4$ or 0.1 M $NaNO_3$. For experiments in CV and RDV, a Princeton Applied Research (PAR) 174 Polarographic Analyzer was used. In rapid scan cyclic voltammetric experiments, a PAR 175 Universal Programmer, a PAR 173 potentiostat, and a Nicolet Explorer I storage oscilloscope were employed with scan rates from 10 mV s^{-1} to 20 V s^{-1}.

Platinum (3.8 mm diameter) and gold (2.2 mm diameter) disk electrodes, and a variable-speed rotator, used in RDV experiments, were manufactured by the Pine Instrument Co., Grove City, Pa. Electrodes were abraded on a polishing wheel, using successively 1.0 μ and 0.3 μ alumina. The scan rate in RDV was typically 5 mV s^{-1}.

Oxidative and reductive controlled-potential electrolysis was under the control of a PAR 173 potentiostat; current measurement and integration were performed by a PAR 179 digital coulometer. The electrolysis cells contained side arms with fine frits, thereby isolating the counter electrode from the working electrode. In CPC experiments, both working and counter electrodes were made of coiled platinum wire. Oxidative electrolyses were ordinarily conducted at 1.1 V *vs.* SSCE, and reductive electrolyses at −0.1 V.

Redox Titrimetry

Oxidative titrations utilized Ce(IV) in 0.5 M H_2SO_4 as the titrant. A typical Ce(IV) concentration was 0.025 M. The platinum-bearing compounds were ordinarily dissolved in 1.0 cm^3 of 1.0 M HCl; without Cl^- the reaction kinetics were intolerably slow. Titrations were monitored potentiometrically using a looped Pt wire as the working electrode and Ag/AgCl as the reference electrode.

Combined CPC/EPR and CPC/Vis Studies

Electrolyses conducted at 1.1 V *vs.* SSCE were sampled during the course of oxidation for examination by visible spectroscopy. 16.0 mg of PtMeU in 6.0 cm^3 of 0.1 M $NaNO_3$ was electrolyzed with 0.5 cm^3 of the solution being removed at each sampling and measured using a Cary 17D spectrophotometer.

For CPC/EPR measurements samples were removed for measurement and immediately frozen down in liquid N_2 until time of analysis (usually later the same day). Spectra were recorded using a Varian E line Century Series spectrometer.

Electrosynthesis of Head-to-Head cis-[$(NH_3)_2$Pt-$(MeU)_2$Pt$(NH_3)_2$]$(ClO_4)_3$, 'Pt(ox)MeU'

The above green compound was most readily obtained if the CPC was carried out in 0.1 M $NaClO_4$ from which it precipitated. Typically 20 mg of PtMeU was electrolyzed in 10 cm^3 of 0.1 M $NaClO_4$. Precipitation of Pt(ox)MeU was complete after the transfer of 1 e^- per molecule of PtMeU. Isolation of Pt(ox)MeU was accomplished by centrifugation of the reaction mixture followed by washing the precipitate with methanol and drying *in vacuo*. Microanalysis of $[(NH_3)_2Pt(MeU)_2Pt(NH_3)_2](ClO_4)_3$ yielded: C; 12.29; H, 2.27; N, 11.46; Cl, 10.49. Calc.: C, 11.93; H, 2.20; N, 11.13; Cl, 10.56%.

Results and Discussion

Cyclic Voltammetry

The cyclic voltammetric behavior of PtMeU over the sweep rate range 10 mV s^{-1} to 500 mV s^{-1} was

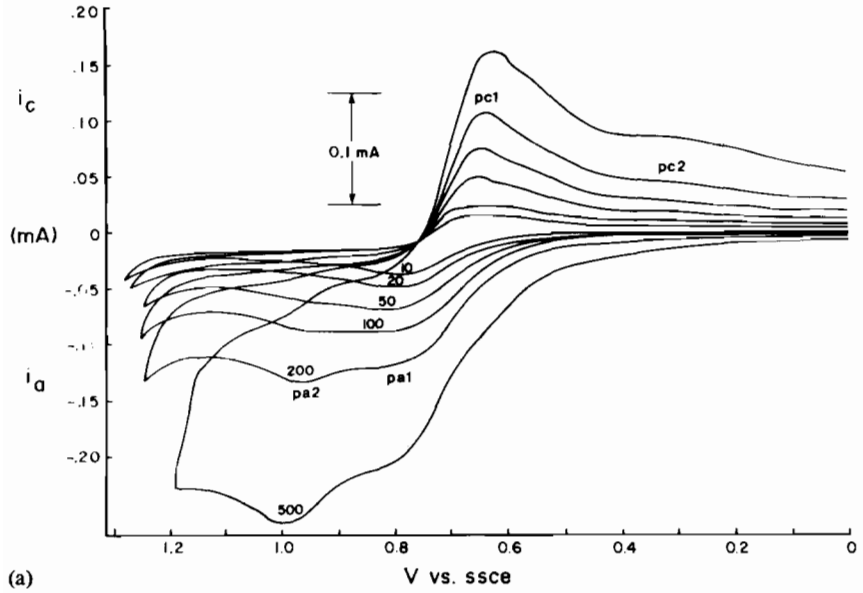

(a)

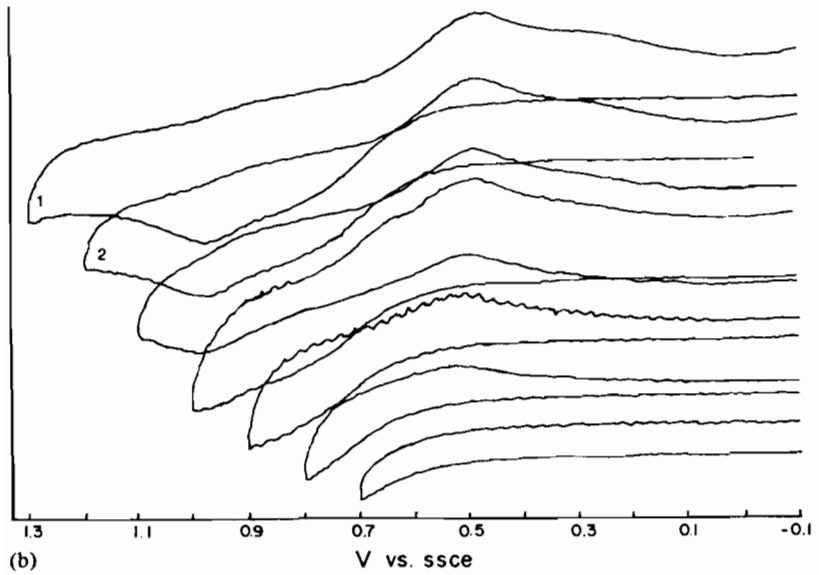

(b)

Fig. 1. (a) Cyclic voltammograms of PtMeU (2.0 mM in 0.1 M $NaNO_3$) at platinum over the sweep rate range ν = 10 mV s^{-1} to 500 mV s^{-1} as labeled; (b) Serial cyclic voltammograms taken at ν = 500 mV s^{-1} demonstrating the correspondence between cathodic and anodic peaks of PtMeU.

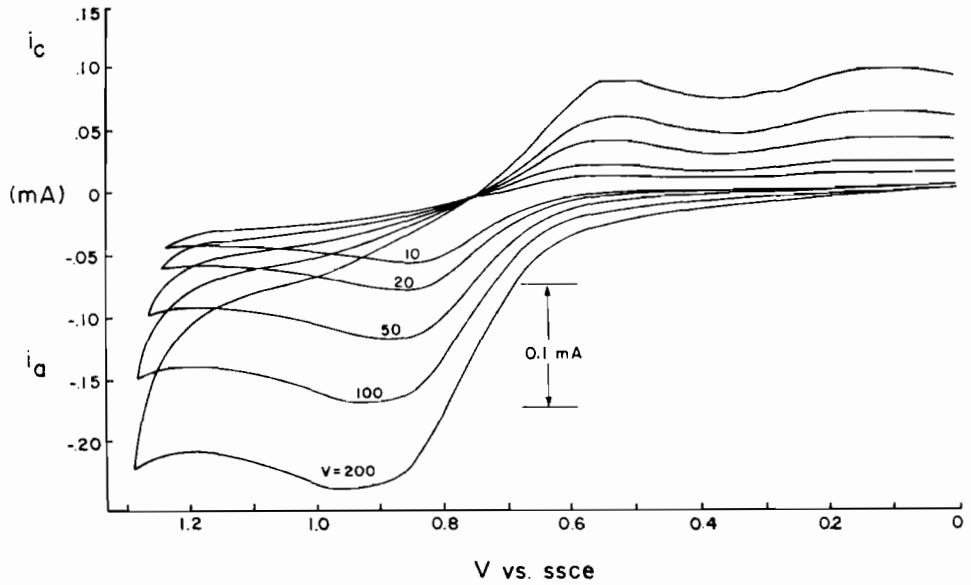

Fig. 2. Cyclic voltammograms of PtMeUB (39 mg in 5.0 cm^3 of 0.1 M $NaNO_3$) at Pt as a function of sweep rate, in the range 10 to 200 mV s^{-1} as labeled.

dependent on the age and condition of the solution. A freshly-prepared solution typically yielded voltammograms at platinum shown in Fig. 1a, while the same solution only hours later yields a less well delineated response, very similar to that of the polymeric PtMeUB shown in Fig. 2. Examination at glassy carbon yielded generally less well-defined curves than at platinum. For example, a second anodic wave, seen for PtMeU at Pt using higher sweep rates (Fig. 1a), is indiscernible at carbon at all sweep rates. Although gold extends the positive potential range by 0.2 V over platinum, voltammograms were virtually identical at platinum and gold. Both PtMeUB and PtMeU exhibited irreversible behavior at mercury, with the apparent reduction of the attached ligands occurring prior to the reduction of divalent platinum to the metal. The +2 state of platinum is apparently highly stabilized in these species [12].

Figure 1a reveals that the CV for PtMeU exhibits an increasingly well-delineated anodic doublet as the scan rate increases. A second peak at 0.96 V emerges at a scan rate of 200 mV s^{-1} which increases to totally engulf the first anodic component for scan rates above 1 V s^{-1} (not shown). In contrast, an unresolved, broad anodic wave is obtained at all scan rates for PtMeUB (Fig. 2). For ease of discussion, we shall label the first and second anodic waves as pa1 and pa2, having peak potentials of E_{pa1} and E_{pa2}; and similarly for the cathodic waves. Comparison of the cathodic responses for PtMeU at the low and high scan rates reveals a broad cathodic wave centered at ~0.33 V (pc2). The less negative cathodic wave (pc1) is centered around 0.64 V and shifts negative with increasing scan rate. Above about 5 V s^{-1} pc1 and pc2 merge into a broad, unresolved wave (not shown). While $\Delta E_{pa} = (E_{pa2} - E_{pa1})$ is on the order of 0.15 V, $\Delta E_{pc} = (E_{pc1} - E_{pc2})$ is somewhat larger, around 0.20–0.23 V. A correspondence between the pairs of peaks pa2 and pc2, and pa1 and pc1 was demonstrated by generating a series of cyclic voltammograms in which the potential of reversal was shifted to less positive potentials in 0.10 V increments (scans initiated at −0.1 V); this is shown in Fig. 1b. Coulometric analysis in conjunction with cyclic voltammetry, presented below, also provides support for this contention. $\Delta E_{pac1} = (E_{pa1} - E_{pc1})$ varied from ~0.13 to 0.15 V as v varied over the range 20–200 mV s^{-1}, ΔE_{pac2} varied from about 0.60 to 0.66 V (v = 100–2000 mV s^{-1}).

At the potential (0 V) at which the scans in Fig. 1a were initiated, both Pt atoms in PtMeU are in the +2 oxidation state. The first wave (pa1) therefore corresponds to the oxidation of Pt(II). By coulometry (discussed below) we show that two electrons are removed per molecule in the oxidation of PtMeU at 1.1 V. It is also seen by combined CPC/EPR measurements (Fig. 3) that a paramagnetic signal arises concomitantly with the oxidation of PtMeU, then vanishes as the electrolysis is completed. This behavior is accounted for by postulating $[Pt(II, III)]^{3+}$ as the intermediate state and $[Pt(III, III)]^{4+}$ as the final product.

Consequently, the CV peak pa1 can be identified with the transition $[Pt(II, II)]^{2+} - e^- \rightarrow [Pt(II, III)]^{3+}$, and pa2 to $[Pt(II, III)]^{3+} - e^- \rightarrow [Pt(III, III)]^{4+}$. We assign the first cathodic peak pc1 to the reduction of remaining $[Pt(II, III)]^{3+}$ to $[Pt(II, II)]^{2+}$, and pc2 in part to $[Pt(III, III)]^{4+} + e^- \rightarrow$

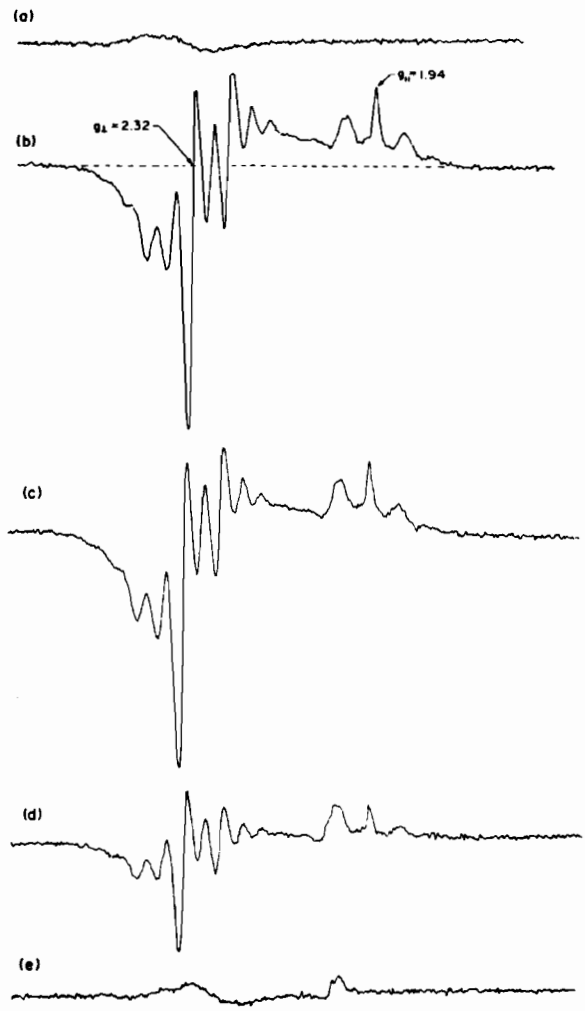

Fig. 3. Frozen solution (−140 °C) EPR spectra of PtMeU in 0.1 M $NaNO_3$; (a) unelectrolyzed, (b) 25% electrolyzed, (c) 50% electrolyzed, (d) 75% electrolyzed, (e) fully electrolyzed. Electrolysis was performed at a potential of 1.1 V; percent electrolysis assumes removal of two electrons (one per platinum atom) for total electrolysis.

$[Pt(II, III)]^{3+}$ with subsequent rapid reduction of the mixed-valence form. Such pairing of pa1 with pc1 and pa2 with pc2, rather than the usual situation pa1 with pc2 and pa2 with pc1, could not of course occur if the second oxidation step were electrochemically reversible.

The high degree of irreversibility of this second step may be due in part to the formation of a surface 'blocking film' formed by the intermediate oxidation product, and whose presence partially blocks access to incoming reactants, thereby impeding further electron transfer. Support for the supposition of a surface film is provided by noting in Fig. 1a that the average number of electrons transferred during an anodic sweep increases with scan rate, as suggested by an increasingly prominent pa2 wave. The preferred explanation for this is that since the surface film is less well developed at the higher sweep rates, surface blockage is less, thereby leading to an enhanced pa2. This is consistent with the observation of a visible green stream, presumably a $[Pt(II, III)]^{3+}$ intermediate, descending from the electrode at the slowest anodic sweep rates employed. In a previous electrochemical study of compounds derived from platinum α-pyridone blue, coupled chemical reactions were postulated to account for similar observations [6]. However, as the CPC/EPR data alluded to above can be accounted for by considering only intermediate oxidation of a binuclear species, we have no cause for invoking the intervention of a chemical step such as, for example, self-association to a tetramer.

It is of interest to compare the CVs of PtMeU with those of related compounds to determine if any others are also explainable in terms of Pt(II)/Pt(III) chemistry. The cyclic voltammogram (not shown) of the mononuclear compound *cis*-$Pt(NH_3)_2(1\text{-}MeU)_2 \cdot 2H_2O$ is readily accounted for in terms of one-step Pt(II) ⇔ Pt(IV) transitions; redox titrimetry corroborated this conclusion. As would be predicted, this mononuclear compound is unable to stabilize the +3 oxidation state. In fact, to the authors' knowledge, only a single, well-authenticated mononuclear Pt(III) complex is known [13]. Another bridged, binuclear platinum compound [14], $[(NH_3)_2Pt(OH)_2Pt(NH_3)_2](NO_3)_2$, yielded no CV at platinum, but did give a sharp, single break typical of the Pt(II) → Pt(IV) transition by redox titrimetry. A review of binuclear Pt(III) complexes reported in the literature reveals that in every case bridging ligands contain sites of unsaturation; hence, this dihydroxo-bridged structure would not be expected to be able to stabilize the +3 state.

It was mentioned above that CVs of aged solutions of PtMeU strongly resembled those of PtMeUB. This was reflected in the following: (1) there was no indication of more than one component to the anodic wave; (2) E_{pa} for the single anodic peak is at more positive potentials; (3) E_{pa} shifts markedly towards more positive potentials with increasing scan rate; (4) pc2 is more prevalent than in the CV of a fresh solution; and (5) at the highest scan rates i_{pc2} is comparable to i_{pc1}. Aqueous solutions of PtMeU could acquire a violet tinge upon standing in contact with air. Further, reversed-phase liquid chromatography of such aged PtMeU solutions suggests that a polymeric distribution not unlike that seen in PtMeUB had formed (Fig. 4). Hence the congeneric relationship of PtMeU to PtMeUB.

The undelineated anodic CV wave characteristic of PtMeUB is not unexpected for a polymeric system bearing interacting metal centers [15]. This is further understandable in terms of the range and variability of oligomeric species that presumably comprise

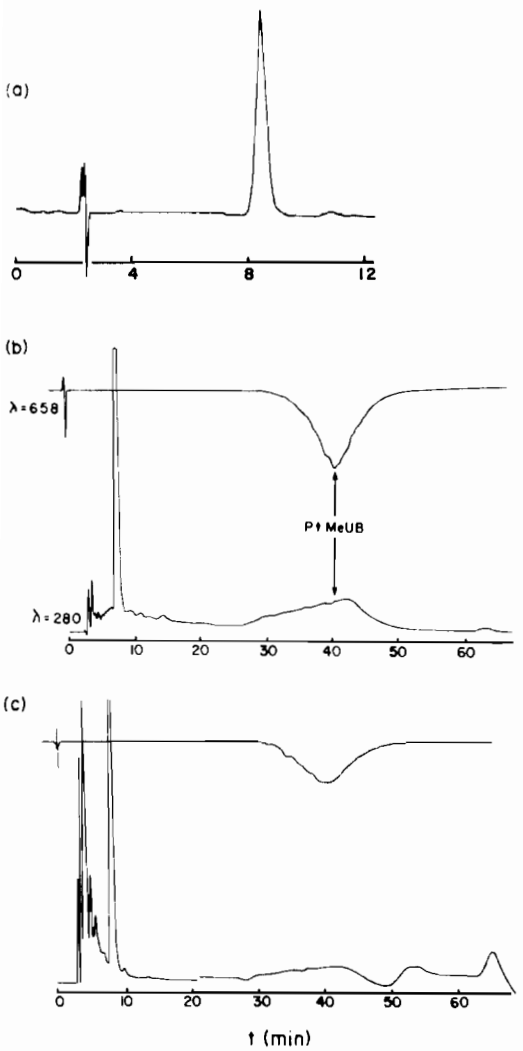

Fig. 4. Ion-pair reversed phase liquid chromatograms (IPR-PLC) of (a) a fresh preparation of PtMeU, 1.0 mg in 10.0 cm^3 of 0.01 M $NaNO_3$, monitored at 280 nm; (b) aqueous solution of PtMeUB, 3.9 mg/5.0 cm^3 of 0.1 M $NaNO_3$; (c) PtMeU aged. The prominent peak at ~7 min in b and c is due to PtMeU. Conditions: column, Partisil ODS-3; (a) eluent, 50% MeOH/0.01 M sodium octylsulfonate/0.005 M tetrabutylammonium (TBA^+) nitrate, pH 3.0 with HNO_3; (b), (c) gradient elution: 100% **A** for 20 min $\xrightarrow{\text{linear}}$ 100% **B** in 30 min (*i.e.*, overall, 50 min program) where **A** is 50% MeOH/0.01 M sodium heptylsulfonate/0.002 M TBA^+, pH 3.0 with HNO_3, and **B** is 80% MeOH/0.008 M ethane sulfonic acid/0.003 M TBA^+.

PtMeUB. Thus, the broad chromatographic band detected at $\lambda = 658$ nm in Fig. 4b suggests a broad distribution of totally unresolved oligomeric components. (It is relevant here to note that O'Halloran and Lippard have documented a slow isomerization of α-pyridonate-bridged ethylenediamineplatinum(II) dimer from the head-to-head to the head-to-tail stereoisomer [16]). The high degree of irreversibility for PtMeUB as indicated by the potential difference between the outer peaks ($\Delta E_{pac2} = 0.85$ V at $\nu =$ 200 mV/s in Fig. 2), is again indicative of highly impeded heterogeneous electron transfer, as for PtMeU.

Rotating Disk Voltammetry

Comparison of the RDVs of PtMeU and PtMeUB showed the rising current in the latter to occur at more positive potentials. The RDV curves of PtMeU show an inflection relating to two discernible electron transfer steps, in harmony with the CV data; no such inflection is discernible in the PtMeUB curves. The voltammetric limiting current for PtMeU oxidation obtained at a freshly polished electrode in comparison with that for the one-electron oxidation of $Ru(NH_3)_6^{2+}$ (a convenient calibration standard) enabled an estimate of n, the number of electrons transferred, to be obtained. Assuming the diffusion coefficients of PtMeU and $Ru(NH_3)_6^{2+}$ to be equal, n values of approximately 1.4–1.9 were obtained over the rotational frequency range 400–5000 rpm. The somewhat lower values from that expected in the absence of complicating factors, $n = 2$, probably arise primarily from surface inhibition effects. A similar comparison by cyclic voltammetry also yielded n values somewhat less than 2, with the exact value being sweep-rate dependent, as already alluded to.

One of the elusive goals of platinum blues chemistry has been the accurate estimation of average molecular weight [17, 18]. A simple, albeit very approximate method of achieving this makes use of rotating disk voltammetry. Given that the net oxidation state of platinum in both PtMeU and PtMeUB is not far from 2, as extracted from controlled-potential coulometry (*vide infra*), the observed ratio of rotating disk limiting currents, i(PtMeUB)/i(PtMeU), for solutions containing equal masses of PtMeUB and PtMeU should approximately equal $[D(\text{PtMeUB})/D(\text{PtMeU})]^{2/3}$, where the Ds are the corresponding diffusion coefficients. This, of course, assumes that the measured currents refer to diffusion-limited conditions so that the Levich equation applies; this was facilitated by employing large anodic overpotentials and making rapid RDV measurements using a freshly polished electrode (*vide infra*). In this calculation the diffusion coefficient of the PtMeU dimer was taken to be the same as that of $Ru(NH_3)_6^{2+}$, 7.5×10^{-6} cm s^{-1}; D for the polymer was calculated to be 1.4×10^{-6} cm s^{-1}. Using an adaptation of the method of Smith *et al.* [19], the corresponding ratio of molecular weights, M, for PtMeUB and PtMeU can be extracted from the Stokes–Einstein equation: $D = 2.96 \times 10^{-7}\ \eta^{-1}\ d^{1/2}\ M^{-1/2}$ where η is the viscosity and d is the solute density. An estimate of M for PtMeUB equal to around 25 000 was obtained in this manner.

Previous studies on other platinum blues using sedimentation analysis and gel electrophoresis have yielded somewhat smaller values of M [4, 17, 18].

Controlled-potential Coulometry

Oxidative electrolysis of PtMeU conducted at 1.1 V yielded an n value equal to 2. During the electrolysis the color proceeded in the fashion colorless → light green → intense green → golden yellow. During the following reduction at −0.1 V the color sequence was slightly different: yellow → green–yellow → light green → colorless; the color did not pass through an intense green. The slight difference in the color progressions may furnish further support for the proposed interpretation of the CVs: because the intermediate $[Pt(II, III)]^{3+}$ is more readily reduced than $[Pt(III, III)]^{4+}$, relatively less of the green product is present in solution during the reductive electrolysis at −0.1 V than during the oxidative electrolysis at +1.1 V. The ln i *vs.* t plots for both the oxidative and reductive electrolysis are linear, thus revealing first-order behavior.

For PtMeUB the oxidative color sequence was deep blue-green → dark green → green–brown → brown–green → brown → honey brown. The reverse order was followed during reductions although the resulting blue–green hue was somewhat paler than the original color. However, the ln i–t plots for PtMeUB were nonlinear, and the currents generally much smaller than those obtained for PtMeU so that the electrolyses of PtMeUB were generally very slow and incomplete. Therefore, an accurate value for n could not be obtained. This is very likely due in part to the tendency of PtMeUB and/or its oxidation products to precipitate onto the electrode surface, to a greater extent than for PtMeU. As noted above, the cyclic voltammetric behavior of both PtMeU and PtMeUB can be ascribed, at least in part, to such surface precipitation. A second likely contributing factor for the slower rate of electrolysis of PtMeUB *vis-a-vis* PtMeU is that in this complex oligomeric species not all Pt(II) centers are oxidized to Pt(III) at comparable rates.

Further evidence for the tendency of, particularly, the polymeric species to precipitate onto or adsorb on the electrode surface was provided by RDV. The relative tendencies of PtMeU and PtMeUB to inhibit further electrode reaction were elucidated by comparing limiting current plateaus for these two species over consecutive runs by RDV made without intervening polishing between runs. While a slight adsorptive effect for PtMeU is evidenced by relatively small reductions in the limiting current upon sequent runs, the progressive diminution of current for PtMeUB was found to be considerable. The higher the rotation speed, in the range 200–3200 rpm, the faster was the observed drop-off in limiting current. This behavior is best accounted for by invoking multilayer adsorption. Thus the net flux to the electrode surface will be diminished even at high overpotentials where the electrode kinetics are rapid if a coherent film is formed, thus restricting access of the incoming reactant to the metal surface.

Estimation of Platinum Oxidation State in PtMeUB

In principle, by comparing the charge accumulated during oxidative and reductive electrolyses of the PtMeUB starting material, where fully oxidized and reduced PtMeUB should contain entirely Pt(III) or Pt(II), respectively, an average formal oxidation state may be assigned to Pt in PtMeUB. As mentioned above, it was not possible to determine accurately the coulombic charge required to entirely oxidize PtMeUB. It was noted that the reductive electrolysis of PtMeUB (conducted at −0.1 V *vs.* SSCE) behaved like an oxidative one, except that the current is considerably lower, presumably a reflection of an average formal oxidation state of PtMeUB being considerably closer to 2 than to 3. If we can assume that the shapes of the oxidative and reductive electrolysis curves for PtMeUB are similar because of the same underlying kinetic factors, then a first-order graphical analysis applied to the early (0–25 min), linear portion of the ln i-*vs.*-t plots should be valid.

When this was performed, values of $Q_{oxid} = 0.846$ C and $Q_{red} = 0.0775$ C were obtained for a solution containing 5.32 mg of PtMeUB. Then Pt(II)/Pt(III) = 0.846/0.0755 ~ 11. This means that, on average, one Pt in 12 is in the +3 valence state, so that the average formal oxidation state of platinum in platinum 1-methyluracil blue is 2.08. This is consistent with the value of 2.08 ± 0.15 reported for a platinum uracil blue (PUB), based on reductive titrimetry, by Lippard *et al.* [4].

Combined Coulometry/Cyclic Voltammetry

Joint CPC/CV studies were performed in order to assess if any irreversible chemical changes accompanied electrolysis. Cyclic voltammograms recorded at 1/8 intervals throughout an exhaustive oxidative electrolysis of PtMeU are shown in Fig. 5. As the electrolysis proceeds (from trace 1 to trace 9), pc2 grows as pc1 subsides. (Note that at the potential of sweep initiation, 0.40–0.44 V, no fully-electrolyzed material undergoes reduction). This behavior is consistent with the above interpretation of the CV peaks. Note that pc2 is composed of at least two discernible components of uncertain origin. Also, the curves pass through an isopotential point in proceeding from pc1 to pc2.

The cyclic voltammograms obtained during reductive electrolysis (Fig. 6, traces 10–17) are not exactly superimposable on their counterparts obtained during oxidative electrolysis. Note particularly the disproportionately large i_{pa}/i_{pc1} ratio in trace 17 compared with trace 1, suggesting a less chem-

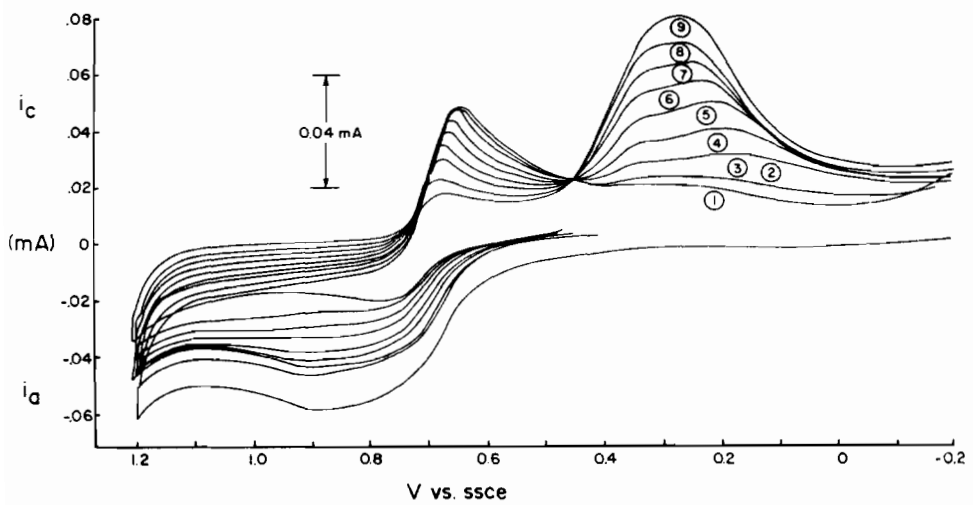

Fig. 5. Cyclic voltammograms of PtMeU (5.7 mg in 6.0 cm^3 of 0.1 M $NaNO_3$) recorded at 1/8 intervals throughout an oxidative electrolysis at 1.1 V; $\nu = 100$ mV s^{-1}. Trace 1 is the CV prior to the electrolysis, trace 9 is following complete electrolysis.

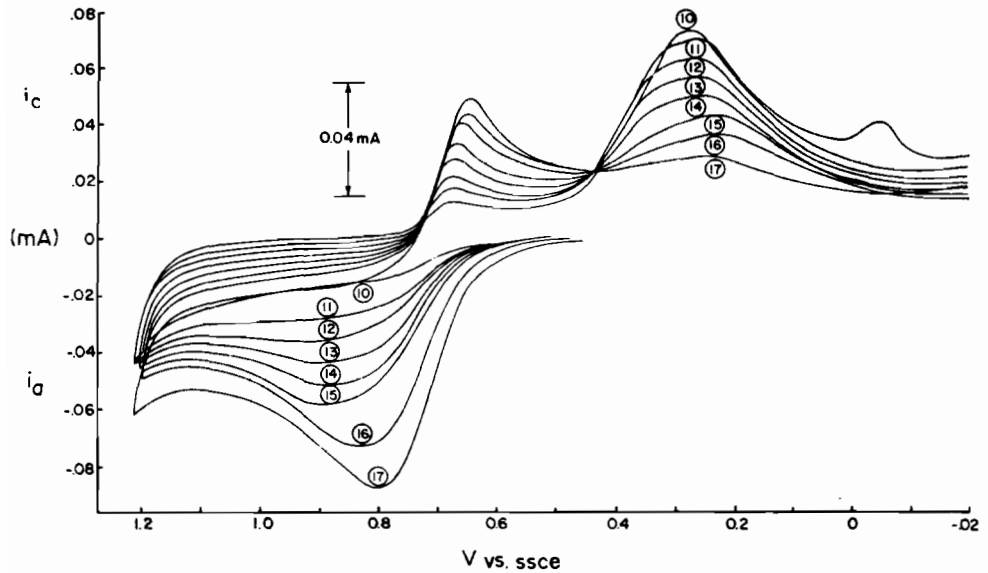

Fig. 6. Cyclic voltammograms of PtMeU obtained during reductive electrolysis at −0.1 V conducted subsequent to the oxidations of Fig. 5; $\nu = 100$ mV s^{-1}. Trace 17 was obtained following complete reductive electrolysis.

ically reversible system immediately after sequential forward and reverse electrolysis compared to the system prior to electrolysis. It is interesting, though, that upon standing undisturbed in the electrolysis cell overnight, a CV virtually identical to trace 1 was nevertheless obtained.

In a separate experiment, exhaustive (4 h) oxidative electrolysis was followed by exhaustive reductive electrolysis (also for 4 h) with only a single CV taken in between (Fig. 7). It is seen that the initial and final CVs are very similar. Hence, the PtMeU redox system is reasonably reversible in a *chemical* sense, even though it exhibits a high degree of *electrochemical* irreversibility.

Similar experiments were conducted on PtMeUB as shown in Figs. 8 and 9. Again, as electrolysis proceeds, i_{pc1} falls, although the effect is less pronounced than for PtMeU. This peak is apparently due to the presence of an impurity as shown by LC (Fig. 4). The second cathodic peak, pc2, is seen to grow under these conditions, the effect now being greater for PtMeUB than for PtMeU. Also E_{pc2} moves towards more positive potentials; this may be the result of the varying influence of two or more

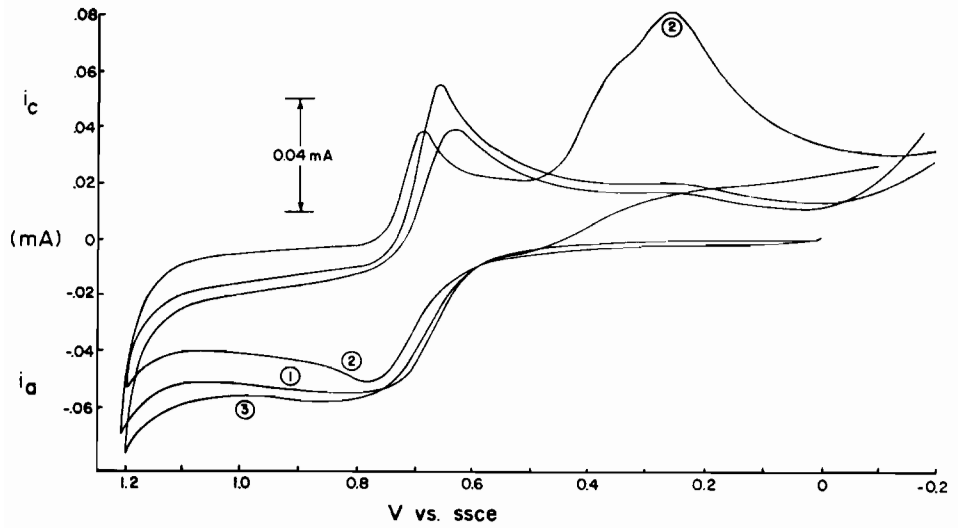

Fig. 7. Cyclic voltammograms conducted at $v = 100$ mV s^{-1} (1) before, (2) between, (3) after oxidative and reductive electrolyses of PtMeU (5.8 mg in 6.0 cm^3 of 0.1 M $NaNO_3$).

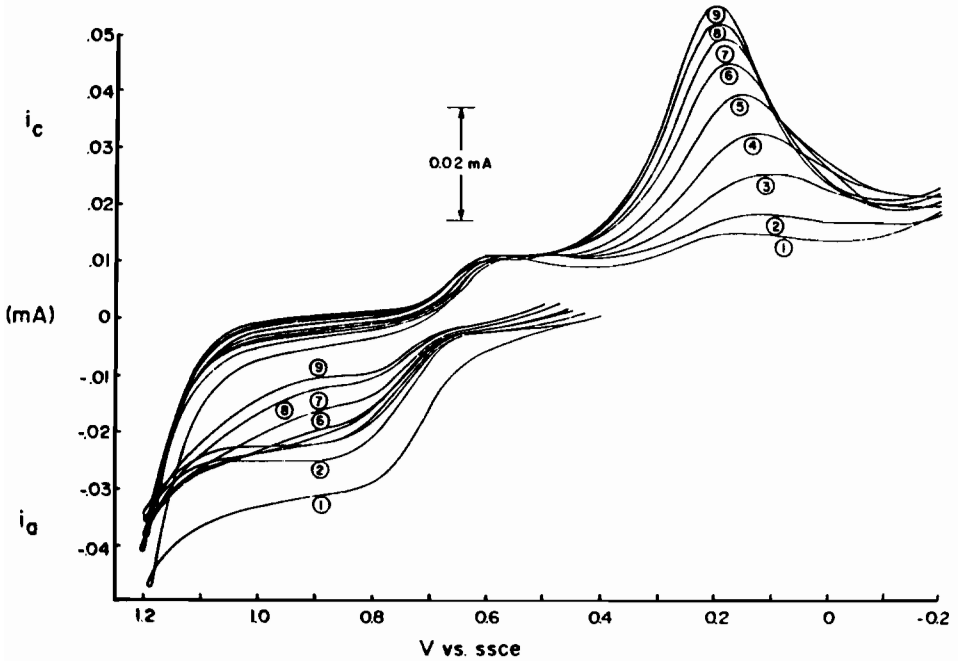

Fig. 8. Cyclic voltammograms of PtMeUB (5.4 mg in 6.0 cm^3 of 0.1 M $NaNO_3$) recorded at 1/8 intervals throughout an oxidative electrolysis conducted at 1.1 V. Trace 1 is the CV prior to electrolysis, trace 9 is the CV following complete electrolysis.

components which together constitute pc2. Overall, E_{pc2} is slightly less positive (by 0.1 V) than for PtMeU. This is primarily a result of the greater electrochemical irreversibility of the platinum blue.

In the reductive electrolysis (Fig. 9, traces 10–17), i_{pa}/i_{pc1} grows to about twice the value it had prior to electrolysis (trace 1, Fig. 8), similar to the situation previously noted for PtMeU. Trace 18 is the CV obtained after the solution stood undisturbed overnight, and matches reasonably well the CV obtained prior to electrolysis. This behavior is very similar to that observed earlier for PtMeU, and again implicates an accompanying chemical change. Based on the greater predominance of pc2 after the sequential electrolyses, it appears that not all of the Pt atoms oxidized to Pt(III) are reduced back to Pt(II). In any event, note that the before-and-after electrolysis match is less definitive than for PtMeU, thus dem-

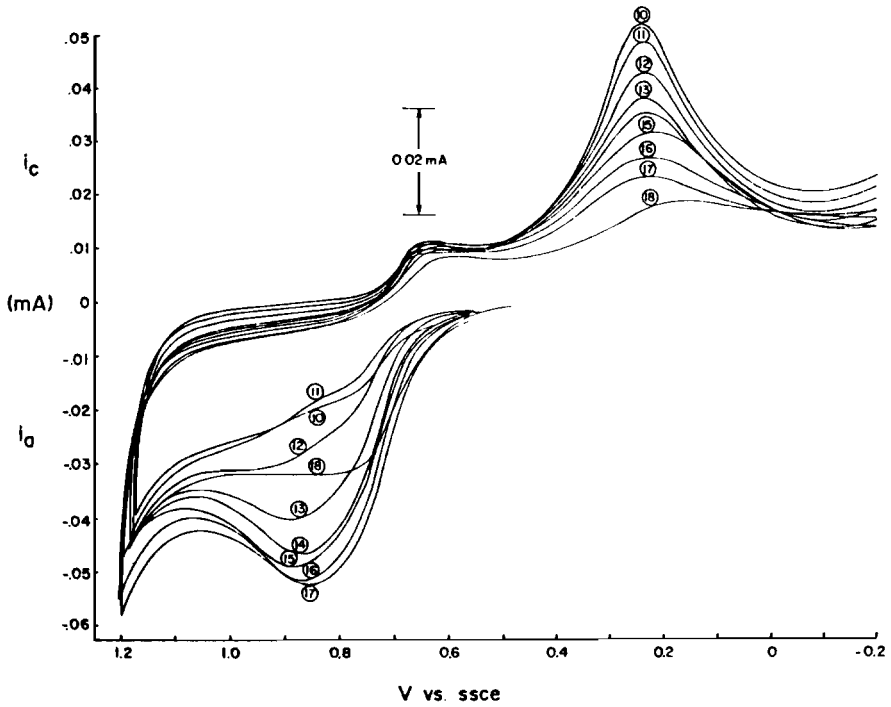

Fig. 9. Cyclic voltammograms of PtMeUB obtained during reductive electrolysis at −0.1 V conducted subsequent to the oxidative electrolysis of Fig. 8. Trace 10 was taken prior to reductive electrolysis, 17 at the conclusion, and 18 after standing overnight.

onstrating the lower reversibility in a chemical sense for the PtMeUB polymer compared to the PtMeU dimer.

Redox Titrimetry

As noted above, complete controlled-potential oxidative electrolysis of PtMeU yielded a number of electrons, n, transferred per molecule equal to two. Given that PtMeU consists wholly of Pt(II), this means that either Pt(III, III) or Pt(II, IV) is the end product. The former possibility is clearly more consistent with the evidence presented above. Regardless of its form, the question may be asked, can further oxidation to a Pt(IV) state be effected? Even though no evidence for a Pt(IV)-containing product was obtained from electrolytic oxidation, such processes may nonetheless occur if chemical oxidants are employed. For the mixed-valent, oligomeric PtMeUB – because of the nonideal electrolysis curves generated – a separate question was, would an equivalence point be discernible? (Certain blues previously examined have yielded ill-defined titration curves [7]). Also, as with PtMeU, if an equivalence point is discernible, and if it can be presumed to correspond to all Pt(III), can further oxidation to Pt(IV) be effected? We addressed these questions by examining the redox chemistry of PtMeU and PtMeUB using the redox reagent Ce(IV). Ce(IV) in 0.5 M H_2SO_4, used here, exhibits a sufficiently positive potential for the Ce(IV)/(III) couple, 1.2 V *vs.* SSCE, so as to provide sufficient oxidizing strength to adequately address these questions.

Wholly unsatisfactory performance was obtained when the titrations were attempted in 4.5 N HCl, as has been earlier reported [7, 20]; unreasonably excessive amounts of Ce(IV) titrant were consumed (due to Cl^- being oxidized) and the titration curves exhibited anomalous behavior, displaying dips. 1 M HCl, used here to dissolve the sample, also makes a small contribution to the blank, but provides a suitable compromise between speed and accuracy; without the addition of chloride, which may serve as a bridge between oxidant and reductant, redox reactions were prohibitively slow, particularly in the vicinity of the end point. To gauge the precision and accuracy of the procedure, we titrated *cis*-$Pt(NH_3)_2Cl_2$ and obtained a mean positive relative error of 7.0 ± 0.4% (for 4 determinations). The error probably stems from the oxidation of Cl^- arising from 1 M HCl used to dissolve the sample.

An end point corresponding to $n = 2$ was obtained for PtMeU, having a positive percent error of 9.7%. This is in agreement with the results of controlled-potential electrolysis, and again implicates either Pt(III, III) or Pt(II, IV) as the end product. Up to the end point, equilibrium was rapidly achieved after the addition of each aliquot of titrant. Beyond the end point, though, the titration began to proceed very slowly, with the potential jumping to a high value immediately upon addition of titrant, and then

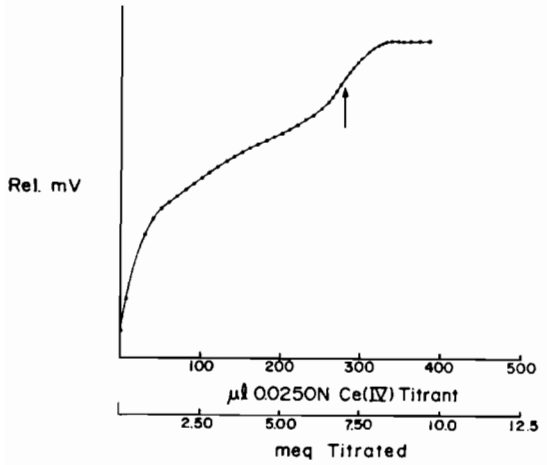

Fig. 10. A titration curve for the Ce(IV) oxidation of PtMeUB; 2.70 mg dissolved in 1.0 cm^3 of 1.0 N HCl, titrated with 0.025 N Ce(IV). The end point was taken at the point arrowed.

slowly drifting towards an equilibrium value. Eventually the drift became intolerably slow, suggesting that further oxidation is occurring, but at a rate much too slow to result in a second break in the curve. (Use of Ce(IV) prepared in HNO_3, a more strongly oxidizing medium, gave similar results.)

A formal potential, E°_f, may be calculated for PtMeU for the half-reaction $[Pt(III, III)]^{4+} + 2e^- \rightarrow [Pt(II, II)]^{2+}$ from its titration curve. It can be shown using Nernstian analysis that for this system $2E^\circ_{f,[Pt(III,III)]} = 3E_{eq} - E^\circ_{f,Ce}$, where E_{eq} is the potential at the equivalence point and $E^\circ_{f,Ce}$ is the formal potential for the $Ce^{4+/3+}$ couple. Carrying through the analysis, a value $E^\circ_f = 0.74$ V *vs.* NHE (0.50 V *vs.* SSCE) was obtained.

The titrimetric behavior of PtMeUB was similar to that of PtMeU, a single end point being obtained (Fig. 10). As the curve flattened out after the equivalence point, the potential reading was 1.0 V, a full 0.3 V below that which would be dictated by the $Ce^{4+/3+}$ couple if no further oxidation was taking place. Again, this is therefore indicative of further oxidation, although as for PtMeU, it was extremely slow.

Combined Coulometry/EPR Studies

In the preceding sections we have alluded to a Pt(II, III) intermediate, Pt(ox)MeU, in the oxidation of PtMeU. The existence of this intermediate was verified, as previously mentioned, by CPC/EPR (Fig. 3) and CPC/Vis studies. We were able to observe the formation and decay of a green (λ_{max} = 742 nm), paramagnetic compound during the oxidation of PtMeU at 1.1 V to its yellow Pt(III, III) analog, which has been isolated as a salt by precipitation with $NaBPh_4$. The green intermediate compound was formed cleanly according to visible spectroscopy with no other absorption bands being observed during the electrolysis.

The maximum concentration of the intermediate was observed (by both techniques) after the removal of 0.4–0.5 electrons per platinum, *i.e.*, slightly earlier than would be anticipated if the conversion is exclusively from Pt(II, II) to Pt(II, III). The reason for this is that the subsequent oxidation to Pt(III, III) occurs simultaneously (it cannot be avoided) as the concentration of the Pt(II, III) species increases during the first half of the electrolysis. The green intermediate solution is due to the presence of the Pt(II, III) mixed-valence species.

We carried out the electrolysis in both 0.02 M $NaClO_4$ and 0.1 M $NaNO_3$ with similar results, except for the hyperfine splitting in the EPR spectrum which is much more pronounced in nitrate solution. By increasing the initial concentration of $NaClO_4$ to 0.1 M we were able to precipitate the green compound from solution during the electrolysis, and after washing with methanol and drying *in vacuo* we obtained an analytically pure sample of *cis*-$[(NH_3)_2Pt(MeU)_2Pt(NH_3)_2](ClO_4)_3$, Pt(ox)MeU, which contains Pt in the average oxidation state of 2.5. The formulation of Pt(ox)MeU as a single species and not as a mixture of different chain length platinum compound is reasonable for a number of reasons. The preparation and properties (including microanalysis) of Pt(ox)MeU were found to be very reproducible. HPLC analysis of Pt(ox)MeU did not reveal the presence of any PtMeUB and its visible spectrum obeys Beer's law with a single absorption at λ = 742 nm; this is not shifted in energy with different counterions.

Apart from the strong absorption in the visible spectrum (ϵ = 5200, 742 nm both as solid and in solution), the mixed valence nature of Pt(ox)MeU is shown by its EPR spectra. In frozen (−140 °C) water, in 0.02 M $NaClO_4$ or as the solid, the EPR of Pt(ox)MeU is a typical anisotropic axial spectrum with $g_\perp = 2.31$ and $g_\parallel = 1.94$ with no hyperfine structure. This behavior parallels that of α-pyridone blue, as does the appearance of fine structure on going to $NaNO_3$ solutions [4b]. For localization to a single platinum (^{195}Pt $I = 1/2$, 33.7% abundance), a 1:4:1 line pattern is expected, whereas if the electron is delocalized over two equivalent platinums (via the d_{z^2} orbitals) a 1:7.9:1:16.5:7.9:1 pattern would be predicted; neither of these situations fits the spectrum observed here. If we assume inequivalent platinums with aPt = 2aPt′ (where a is the hyperfine coupling constant and Pt and Pt′ refer to the two inequivalent platinum atoms), then a spectrum of approximate distribution 1:4:5:16:5:4:1 is expected. This is close to the observed spectrum, and although not a perfect fit, seems reasonable bearing in mind the difficulties encountered in analyzing these types of data.

A very weak EPR spectrum is obtained for PtMeUB, thus demonstrating that platinum 1-methyluracil blue is only weakly paramagnetic. This result tends to corroborate our earlier conclusion that the average formal oxidation state in PtMeUB is close to 2. Since, as indicated, we believe there to be roughly 11 Pt(II) sites for every Pt(III), considerable delocalization of an unpaired electron is to be expected in the polymer. The application of second-order perturbation effects in the calculation of g values supports greater delocalization in PtMeUB than in Pt(ox)MeU. In general, the same arguments invoked to interpret the EPR spectrum of Pt(ox)MeU can be applied in the case of PtMeUB, although in a somewhat less rigorous fashion because the overall symmetry is lower. The spectrum is again that of an axially-symmetric system containing both parallel and perpendicular orientations. g Values of $g_\perp = 2.275$ and $g_\parallel = 1.948$ are, as with the dimer, indicative of considerable spin–orbit coupling. They further imply that the unpaired electron(s) is primarily associated with overlapping $5d_{z^2}$ atomic orbitals along the Pt axis of the oligomeric chain. Hence, these results support the generally-held view that platinum blues consist of a columnar stacking of Pt units.

Acknowledgements

This work was performed with the aid of Professor B. Rosenberg, and was supported in part by the Air Force Office of Scientific Research (via a grant to M.J.W.).

References

1 J. P. Davidson, P. J. Faber, R. G. Fischer, Jr., S. Mansy, H. J. Peresie, B. Rosenberg and L. Van Camp, *Cancer Chemother. Rep., Part 1, 59*, 287 (1975).
2 R. J. Speer, H. Ridgeway, L. M. Hall, D. P. Stewart, K. E. Howe, D. Z. Lieberman, A. D. Newman and J. M. Hill, *Cancer Chemother. Rep., 59*, 629 (1975).
3 B. Rosenberg, *Interdiscipl. Sci. Rev., 3*, 1 (1978).
4 (a) J. K. Barton, D. J. Szalda, H. N. Rabinowitz, J. V. Waszezak and S. J. Lippard, *J. Am. Chem. Soc., 101*, 1434 (1979); (b) J. K. Barton, C. Caravana and S. J. Lippard, *J. Am. Chem. Soc., 101*, 7269 (1979).
5 P. K. Mascharak, I. D. Williams and S. J. Lippard, *J. Am. Chem. Soc., 106*, 6428 (1984).
6 (a) L. S. Hollis and S. J. Lippard, *J. Am. Chem. Soc., 103*, 6761 (1981); (b) L. S. Hollis and S. J. Lippard, *Inorg. Chem., 22*, 2605 (1983).
7 M. P. Laurent, J. C. Tewksbury, M.-B. Krogh-Jespersen and H. Patterson, *Inorg. Chem., 19*, 1656 (1980).
8 J.-P. Laurent, P. Lepage, P. Castan and P. Arrizabalaga, *Inorg. Chim. Acta, 67*, 31 (1982).
9 J. K. Barton and S. J. Lippard, *Ann. N.Y. Acad. Sci., 313*, 686 (1978).
10 J. D. Woollins and B. Rosenberg, *J. Inorg. Biochem., 19*, 41 (1983).
11 A. J. Bard and L. R. Faulkner, 'Electrochemical Methods, Fundamentals and Applications', Wiley, New York, 1980.
12 R. N. Goldberg and L. G. Hepler, *Chem. Rev., 68*, 229 (1968).
13 R. Usón, J. Forniés, M. Tomás, B. Menjón, K. Sünkel and R. Bau, *J. Chem. Soc., Chem. Commun.*, 751 (1984).
14 R. Faggiani, B. Lippert, C. J. L. Lock and B. Rosenberg, *J. Am. Chem. Soc., 99*, 777 (1977).
15 J. B. Flanagan, S. Margel, A. J. Bard and F. C. Anson, *J. Am. Chem. Soc., 100*, 4248 (1978).
16 T. V. O'Halloran and S. J. Lippard, *J. Am. Chem. Soc., 105*, 3341 (1983).
17 B. Lippert, *J. Clin. Hematol. Oncol., 7*, 26 (1977).
18 A. J. Thompson, I. A. G. Roos and R. D. Graham, *J. Clin. Hematol., 7*, 242 (1977).
19 T. W. Smith, J. E. Kuder and D. Wychick, *J. Polym. Sci., 14*, 2433 (1976).
20 C. A. Chang, R. B. Marcotte and H. H. Patterson, *Inorg. Chem., 20*, 1632 (1981).